ELSEVIER

Computational Materials Science 26 (2003) 61–70

COMPUTATIONAL MATERIALS SCIENCE

www.elsevier.com/locate/commatsci

Strain localization phenomena under cyclic loading: application to fatigue of single crystals

S. Flouriot *, S. Forest, L. Rémy

Centre des Matériaux/UMR 7633, Ecole des Mines de Paris/CNRS, BP 87, 91003 Evry Cedex, France

Abstract

Kinematic hardening plays an important role in strain localization phenomena under cycling loading. A single crystal constitutive model including non-linear kinematic hardening is presented. Using a heterogeneous distribution of kinematic hardening variable in a single crystal plate, a continuum model for the formation of intrusion/extrusion is proposed based on FE simulation. The attention is focused on ratchetting phenomena taking place in the localization band. A second example of strain localization is shown by the strain field at the crack tip in single crystals. 2D and 3D finite element computations of the crack tip field in a CT specimen are provided. They are compared to analytical solutions. The 3D computations show that slip activity is different in the bulk or at the surface of the specimen. The evolution of the crack tip field subjected to cyclic loading is investigated. Ratchetting phenomena are shown to take place in some of the localization bands.

Keywords: Single crystal; Fatigue; Localization; Ratchetting; Crack

1. Introduction

The bifurcation criteria originally proposed in [1] have been used successfully in many situations to predict the occurrence of strain localization in elastoplastic solids, mostly under monotonous loading. The orientation of shear bands can be predicted with good accuracy for geomaterials or metals, including anisotropic materials like single crystals [2]. In contrast, contributions for predicting localization modes under cyclic loading are much less numerous [3]. The aim of the present work is to illustrate two types of localization modes under cyclic loading: formation of extrusion/intrusion bands and ratchetting phenomena in localization bands at a crack tip. Both phenomena are frequently observed especially in the cyclic deformation of metallic single crystals.

Fatigue in Cu single crystals has been studied by many authors [4]. Sectioned surfaces of a fatigued Cu single crystal reveal so-called persistent slip bands. Plastic deformation is then localized in slip bands that form extrusions at the surface. Fatigue cracks can initiate in such deformation bands [5]. In Ni-base single crystal superalloys, intense slip lines appear on the surface of the specimen during cycling. Hanriot [6] observed heterogeneous deformations at low temperature. In Fig. 1 a first intense slip band appeared during

* Corresponding author.

0927-0256/02/$ - see front matter © 2002 Published by Elsevier Science B.V.
PII: S0927-0256(02)00393-2

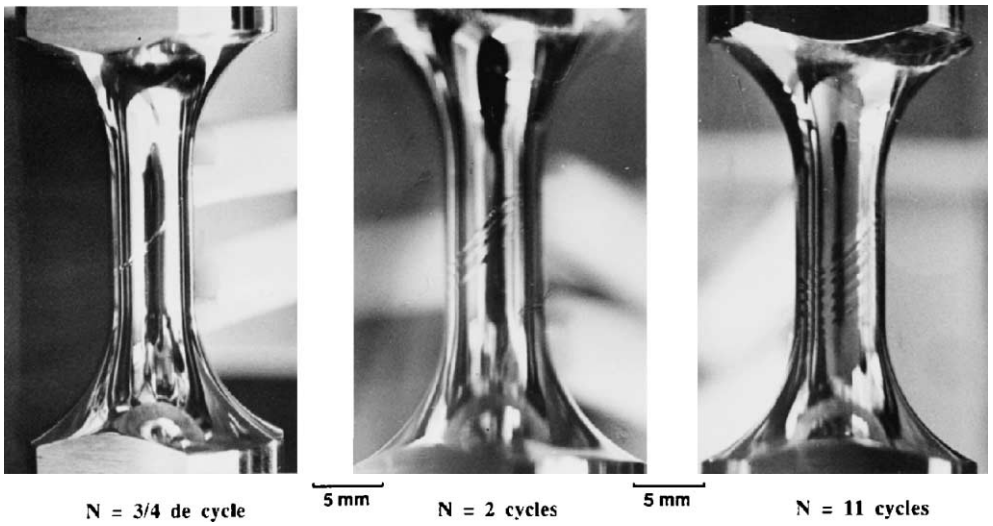

Fig. 1. Strain localization on the surface of a Ni-base single crystal. The test is carried out at 20 °C under total axial strain control ($\Delta\epsilon_p = 2 \times 10^{-3}$) on a polished low cycle fatigue specimen. The number of slip bands increase with the number of cycles. (After [6].)

the first tensile loading, a second during the reverse loading. The number of slip bands increases with the number of cycles until the whole specimen is covered. Such bands may well be the precursor of fatigue damage.

Another example of strain localization in single crystals is given by the strain field predicted at the crack tip in a single crystal [7]. Sectors of constant stress limited by strain localization bands are expected. In the present work, the evolution of these bands under cyclic loading is investigated.

For that purpose, a single crystal constitutive model including non-linear kinematic hardening is presented. It is applied to the simulation of localization bands appearing under cyclic loading. A continuum model for the formation of extrusions, based on the use of a heterogeneous distribution of a kinematic hardening variable is proposed. In the third part, 2D and 3D finite element computations of the crack tip fields in a single crystal CT specimen are provided. They are compared to available analytical solutions. Ratchetting phenomena are shown to take place in some deformation bands when the specimen is subjected to cyclic loading.

2. Strain localization in a single crystal under cycling loading

2.1. Single crystal model

The model used in this work to describe the elasto(visco)plastic behavior of f.c.c single crystals has been developed in [8]. It is based on crystal plasticity theory at small strains. The total strain is partitioned into an elastic and a plastic part

$$\boldsymbol{\varepsilon} = \boldsymbol{\varepsilon}^{\mathrm{e}} + \boldsymbol{\varepsilon}^{\mathrm{p}}, \quad \boldsymbol{\sigma} = \mathbf{C} : \boldsymbol{\varepsilon} \tag{1}$$

where $\mathbf{C}$ is the fourth-rank tensor of elastic moduli. Plastic deformation is the result of slip processes according to 12 octahedral slip systems

$$\dot{\boldsymbol{\varepsilon}}^{\mathrm{p}} = \sum_{g=1}^{12} \boldsymbol{m}^g \dot{\gamma}^g \quad \text{with} \quad \boldsymbol{m}^g = \tfrac{1}{2}(\boldsymbol{l}^g \otimes \boldsymbol{n}^g + \boldsymbol{n}^g \otimes \boldsymbol{l}^g) \tag{2}$$

where $\boldsymbol{l}^g$ is the glide direction and $\boldsymbol{n}^g$ the normal to the slip plane, for slip system g. The amount of slip rate $\dot{\gamma}^g$ is given by

$$\dot{\gamma}^g = \left\langle \frac{|\tau^g - x^g| - r^g}{k} \right\rangle^n \operatorname{sign}(\tau^g - x^g) \tag{3}$$

where $\tau^g = \boldsymbol{\sigma} : \boldsymbol{m}^g$ is the resolved shear stress. For each slip system, internal variables are introduced to describe the hardening of the material: isotropic hardening variable r^g and kinematic hardening variable x^g. The flow rule (3) is used in this work near its rate-independent limit associated with large values of parameters n or $1/k$. The non-linear evolution rule for isotropic hardening involves an interaction matrix H^{gr} which is settled to identity in this work as in [8]:

$$r^g = r_o + Q\sum_r H^{gr}(1 - \mathrm{e}^{-bv^r}) \quad \text{with} \quad \dot{v}^r = |\dot{\gamma}^r| \tag{4}$$

The following form of non-linear kinematic hardening is adopted

$$\dot{x}^g = c\dot{\gamma}^g - \dot{v}^g d(x^g - \bar{x}) \tag{5}$$

The second term in the right-hand side of the equation is the non-linear part associated to the irreversibility of the to and fro dislocation motion (in particular possible change of plane during reverse motion). The additional constant term $\bar{x}$ introduces a tension–compression asymmetry observed in nickel-based superalloys at specific temperatures. The integration of Eq. (5) under monotonous tensile (+) or compressive (−) loading for a crystal undergoing single slip, gives

$$x = \left(\bar{x} \pm \frac{c}{d}\right)(1 - \mathrm{e}^{\mp d\gamma}) \tag{6}$$

2.2. Kinematic hardening and ratchetting effect

Non-linear kinematic hardening is the main ingredient to model the irreversibilities of cyclic slip. It corresponds to a "back-stress" due to polarized dislocation distributions [9]. The internal stresses resulting in strain hardening are produced by dislocation pile-ups for instance. A direct link between such dislocation configurations and linear kinematic hardening is provided in [9]. As for him, Asaro [10] proposes micromechanical arguments for three kinds of kinematic hardening. The applied stress is a function of internal structure variables $\sigma = \sigma(\alpha_1, \alpha_2, \alpha_3, \ldots)$ determining the flow strength. The order in which the recovery of individual events α_i occurs during reverse loading determines the type of kinematic hardening. The first kinematic hardening scheme corresponds to the reverse sequence $2\alpha_1$, $2\alpha_2$, $2\alpha_3$, the second to the order α_1, α_2, α_3 and the third to α_3, α_2, α_1. The formulation of kinematic hardening used in this work is related to Asaro's third mechanism.

The formation of an extrusion or an intrusion in a metal grain is modelled in [9,11] by dislocation pile-ups on two neighbouring plastically deformed layers with the assumption of irreversible dislocation motion. One pile-up forms during tensile loading. It induces a negative back-stress in the vicinity of the first layer (I). Therefore during reverse loading, plastic flow will occur near the first one (layer II). As a result, further plastic deformation takes place on layer I during tension and on layer II during the compressive part of the cycles. Extensions of this simple model of extrusion/intrusion phenomenon can be found in [12]. In the derivation, kinematic hardening plays the central role. The progressive accumulation of plastic slip in each band, cycle after cycle, can be regarded as a ratchetting phenomenon. Constitutive models accounting for ratchetting from a macroscopic point of view under uniaxial or multiaxial loading are available [13] and can help designing the proper evolution equation at the single crystal level. This is the case for Eq. (5) which represents, in a rather phenomenological way, the reversible and irreversible parts of the go and fro motion of underlying dislocations. The modelling of ratchetting effects requires non-zero mean stress and non-linear kinematic hardening.

2.3. Finite element simulations

Strain localization phenomena in single crystals under monotonous loading have been extensively studied from both a theoretical and a numerical point of view [2,14]. Bifurcation analyses show that strain softening is required for localization to occur at the early stage of plastic flow. One usually considers a single crystal plate in tension with a slight initial material or geometric flaw to trigger localization. Shear band formation occurs at or slightly after the peak of the load–displacement curve. If the single crystal plate is then subjected to

cyclic tension–compression, the whole deformation will take place in the formed shear band. No additional band will form. If the material can cyclically harden, the band will thicken and spread over the entire sample. This type of modelling, well suited for localization under monotonous loading, is therefore not sufficient to obtain extrusion or intrusion formation.

To obtain multiple slip band formation, we propose to assume that the plate is initially, or after some cycles, slightly inhomogeneous. For simplicity, the plate, oriented for plane single slip, is divided into two parts: the upper (resp. lower) part has an initial positive (resp. negative) $\bar{x}$ component. The value of the parameters used in the simulation are given in Table 1. Isotropic softening is introduced via a negative parameter Q in 4. The intrinsic response of each individual part in shown by the stress–strain loops of Fig. 2. Due to the presence of parameter $\bar{x}$, the loops are not symmetric in stress. A material imperfection is introduced in each part. The peak of the stress–strain curve is reached earlier in the lower part of the plate than in the upper one during the first tension. As a result, a first slip band appears (Fig. 3, $N = 1/2$ cycle). During the following compressive stage, a second slip band forms in the upper part (Fig. 3, $N = 1$ cycle). During the subsequent cycles, the upper (lower) band is active only during compression (resp. tension). This results in the formation of an extrusion/intrusion between the two slip bands (Fig. 3, $N = 4, 8$ cycles). The amplitude of the extrusion increases with the number of cycles. Fig. 4a shows the global mechanical response of the plate. The overall strain–stress curve is symmetric although the local response of each crystal element is not. The local strain–stress in a slip band displays a ratchetting effect in the slip band (Fig. 4b).

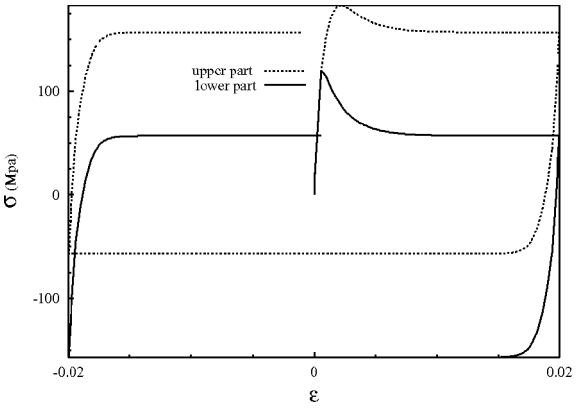

Fig. 2. Single crystal intrinsic behavior obtained for one tension–compression cycle with the material parameters of Table 1.

3. Cracks in single crystals

The purpose of this part is to present the strain and stress fields at a stationary mode I crack tip in an elastic-perfectly plastic f.c.c. single crystal. The attention is focused on the three-dimensional field in a CT specimen and on its local cyclic response.

3.1. Asymptotic solution

An asymptotic solution of crack tip stress fields has been proposed in [7,15] for plane strain tensile (mode I) crack in elastic-ideally plastic single crystals. It is shown that angular sectors with constant stress exist around the crack tip. The shear discontinuities between sectors can be interpreted as strain localization bands which can be slip or kink bands. Drugan [16] has derived other crack tip deformation fields which do not require the existence of kink bands. Rice [7] considers (0 1 1)[1 0 0] and (1 0 0)[0 1 1] cracks for f.c.c. and

Table 1
Material parameters used in the simulation of strain localization in a single crystal plate under cyclic loading

	Elasticity		Isotropic hardening			Kinematic hardening		
	E (MPa)	v	R_0 (MPa)	Q (MPa)	b	C (MPa)	D	$\bar{x}$ (MPa)
Upper part	200,000	0.3	50	−30	210	20,000	900	+20
Lower part	200,000	0.3	50	−30	210	20,000	900	−20

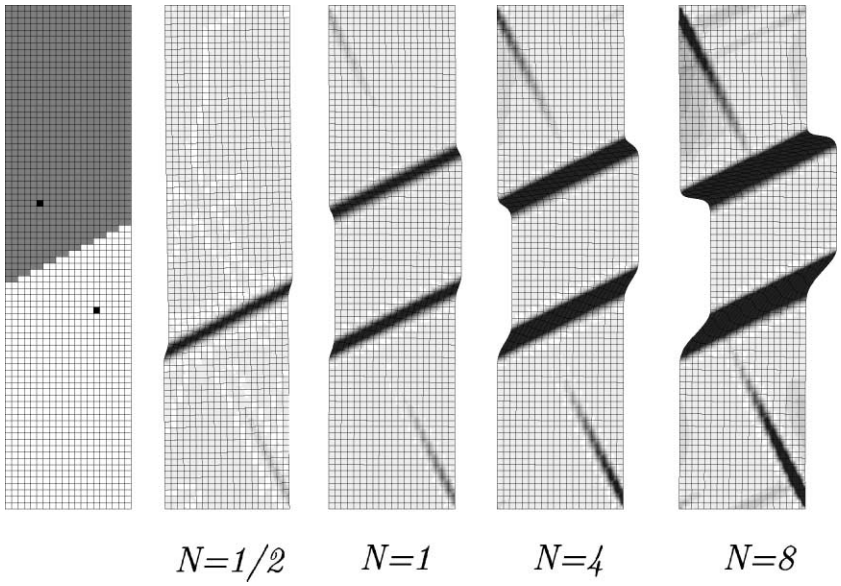

Fig. 3. Strain localization in a plate oriented for single slip: representation of the two inhomogeneous parts of the crystal and location of the imperfections (left), slip band and extrusion/intrusion formation during the first eight cycles (black corresponds to more that $\gamma = 0.1$).

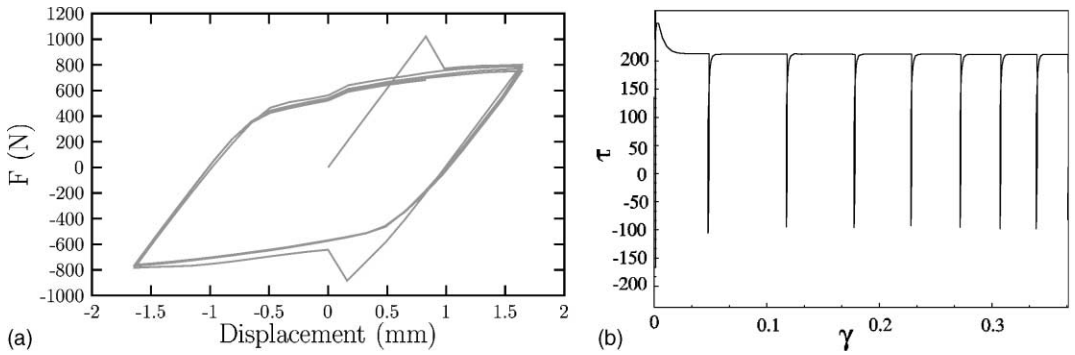

Fig. 4. Single crystal plate in tension–compression: (a) overall response, (b) ratchetting effect in a localization band.

b.c.c. crystals. The notation ( ) denotes the crack plane and [ ] the crack propagation direction. In the present work, we consider also the orientation (0 0 1)[1 0 0] which gives a different deformation pattern at the crack tip. The Cartesian axes 1 and 2 of the crack of Fig. 5b then coincide with crystal directions [0 0 1] and [1 0 0] respectively. Necessary condition for slip to occur is that the resolved shear stress on a slip system reaches the critical value: $\tau^g = \tau_c$. The yield surface can be represented as a curve in the stress space of $((\sigma_{11} - \sigma_{22})/2, \sigma_{12})$.

For elastic–plastic materials the same result can be applied to the stress state in a large sustained strain. The yield surface for the studied orientation is shown in Fig. 5a in the stress space $((\sigma_{11} - \sigma_{22})/2, \sigma_{12})$. Every facet corresponds to a family of activated slip systems. The equation of the yield surface can be written in the form

$$N_\alpha \sigma_{\alpha\beta} S_\beta = b\tau_c, \quad \text{or}$$

$$2N_1N_2\frac{\sigma_{11} - \sigma_{22}}{2\tau_c} + (N_1^2 - N_2^2)\frac{\sigma_{12}}{\tau_c} = b \tag{7}$$

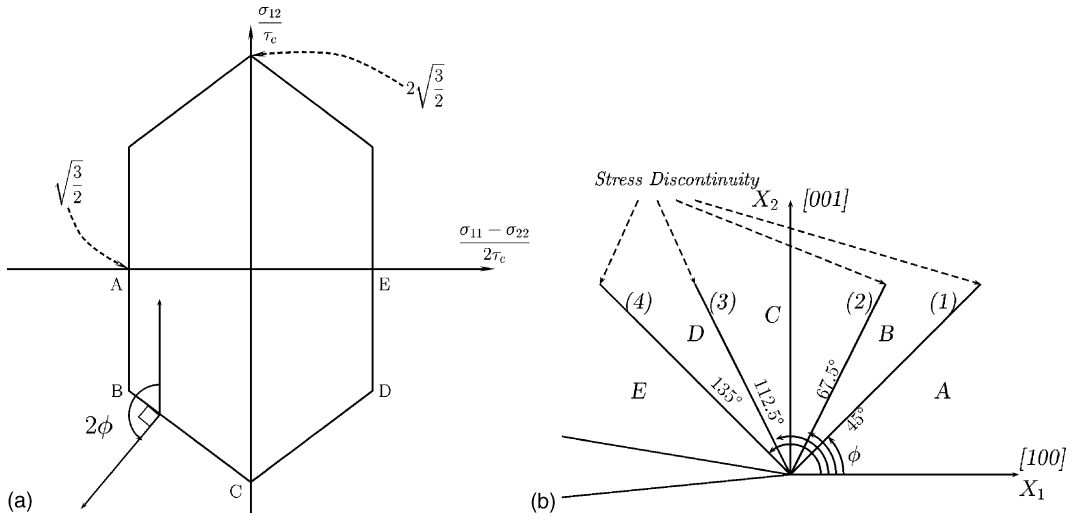

Fig. 5. (a) Yield surface for a (0 0 1)[1 0 0] crack, (b) asymptotic structure of the crack tip.

where N_α and S_α are the unit normal and tangent vectors of a family of slip plane traces in the straining plane (0 1 0). A polar coordinate system r, θ centered at the crack tip, so $x_1 = r\cos\theta$, $x_2 = r\sin\theta$ is introduced. Rice [17] and Drugan [18] have shown that the asymptotic equilibrium requires

$$\sigma'_{\alpha\beta} = e_\alpha e_\beta(\sigma'_{11} + \sigma'_{22}) \quad \text{with} \quad ()' \equiv \lim_{r\to 0} \frac{\partial()}{\partial\theta} \tag{8}$$

Here $e_\alpha = \partial r/\partial x_\alpha$ with $\boldsymbol{e}_1 = (\cos\theta, \sin\theta)$ is the radial unit vector in the x_1, x_2 plane. Combining this equation with Eq. (7), we get

$$(N_\alpha e_\alpha)(N_\beta e_\beta)(\sigma'_{11} + \sigma'_{22}) = 0 \tag{9}$$

This equation shows that the Cartesian stress component is constant in each plastic sector except for special angle θ for which $\mathbf{e}$ is collinear to $\boldsymbol{N}$ or $\boldsymbol{S}$. In our case we have four values of θ associated with a stress jump. The continuity of the traction vector across each sector boundary leads to an additional equation

$$[\![\tfrac{1}{2}(\sigma_{11} + \sigma_{22})]\!] = -[\![L]\!] \tag{10}$$

where L is the arc length along the yield surface measured in the counterclockwise sense. For the crack orientation (0 0 1)[1 0 0] the stress components are given in Table 2. The orientations of the discontinuity lines are given in Fig. 5b.

3.2. 2-D finite element analysis

Numerical analysis of a (0 0 1)[1 1 0] crack in single crystals has been performed and compared to the analytical prediction in [15,19] in finite strain crystal plasticity.

We present here the case of a CT specimen with a (0 0 1)[1 0 0] crack. Only one half of the specimen

Table 2
Stress distribution for a (0 0 1)[1 0 0] crack

Stress	Angular sectors				
	A	B	C	D	E
	0°/45°	45°/67.5°	67.5°/112.5°	112.5°/135°	135°/180°
σ_{11}/τ_c	$(2+2\sqrt{2})\sqrt{3/2}$	$(1+2\sqrt{2})\sqrt{3/2}$	$(2+\sqrt{2})\sqrt{3/2}$	$3\sqrt{3/2}$	$2\sqrt{3/2}$
σ_{22}/τ_c	$(4+2\sqrt{2})\sqrt{3/2}$	$(3+2\sqrt{2})\sqrt{3/2}$	$(2+\sqrt{2})\sqrt{3/2}$	$\sqrt{3/2}$	0
σ_{12}/τ_c	0	$-\sqrt{3/2}$	$-\sqrt{3/2}$	$-\sqrt{3/2}$	0

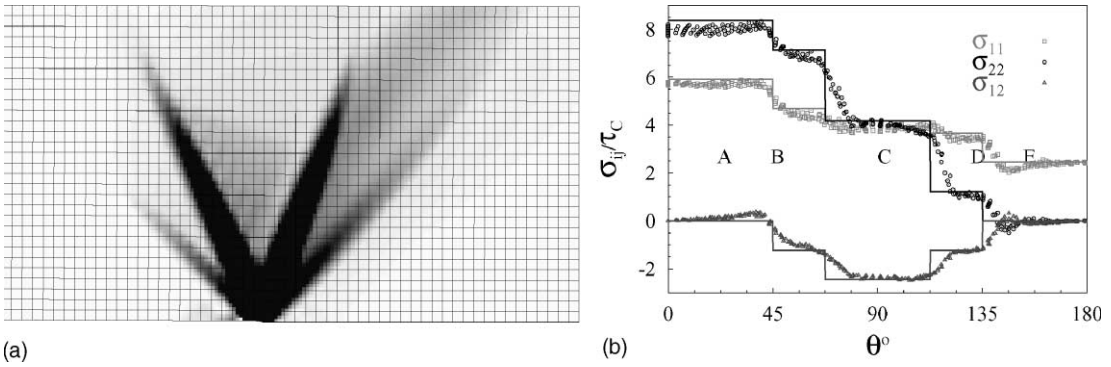

Fig. 6. (0 0 1)[1 0 0] crack: (a) strain localization at the crack tip, (b) stress profiles along a circular line at a given distance from the crack tip and parametrized by polar angle θ.

is considered. A regular mesh with quadratic elements is used at the crack tip. The single crystal model of Section 2.1 is used, without hardening (elastic ideally plastic behavior). Fig. 6a shows the four localization bands found at the crack tip. The numerical solution agrees with the analytical prediction, as shown in Fig. 6b, which gives the stress profile along a circular arc near the crack tip. It has been checked that the use of finite strain crystal plasticity does not significantly affect this result. This localization pattern has been described in [20]: The localization bands (1) at 45° and (4) at 135° is composed of superimposed slip and kink bands. Localization bands (2) and (3) at 67.5° and 122.5° are more complex multislip bands.

3.3. 3-D finite element analysis

Experimental techniques for the determination of near-tip deformation fields rely on surface measurements. For example Shield and Kim [21] and Crone and Shield [22] have measured deformation field using Moiré interferometry which allows precise determination of strain fields in single crystals. Glide shear sector boundaries were observed. But Moiré Interferometry measures the strains on a free surface, which is not under plane strain condition. The asymptotic solution and the 2D FE analysis are only valid for plane strain, i.e. in the interior of the specimen. Three-dimensional near-tip fields in a copper single crystal specimen loaded in four-point bending have been computed in [23]. Slip activity at the surface and the interior is found to differ significantly.

That is why surface effects are investigated here for the CT specimen. Owing to the symmetry of the problem, only one quarter of the CT specimen is considered (Fig. 7). Both orientations (0 0 1)[1 0 0] and (0 0 1)[1 1 0] are considered. Due to the large number of degrees of freedom (270,000), it has been resorted to parallel computing (see [24] for more details on the parallel computation method). Fig. 7 shows the mesh of the CT specimen and the 3D crack tip fields for both investigated orientations. For the (0 0 1)[1 1 0] orientation, in the core of the specimen, three localization bands appear in agreement with the analytical prediction. In contrast, only one localization band is found at the surface, in which one slip system ($[1\,1\,\bar{1}](1\,1\,0)$) is dominant. This system induces out-of-plane plastic flow (Fig. 8).

3.4. Cyclic loading

The evolution of the stress–strain field at the crack tip during cyclic deformation is investigated for a (0 0 1)[1 1 0] CT specimen under plane strain conditions. Contact conditions in the case of crack closure are accounted for. Three localization bands appear during the first tensile loading (as in Fig. 9). In the first band (1) (at 55°) two slip systems are activated simultaneously with the same amount of slip and result in a $(1\,1\,\bar{1})[1\,1\,2]$ effective slip system. The second band (2) (at 90°) can be

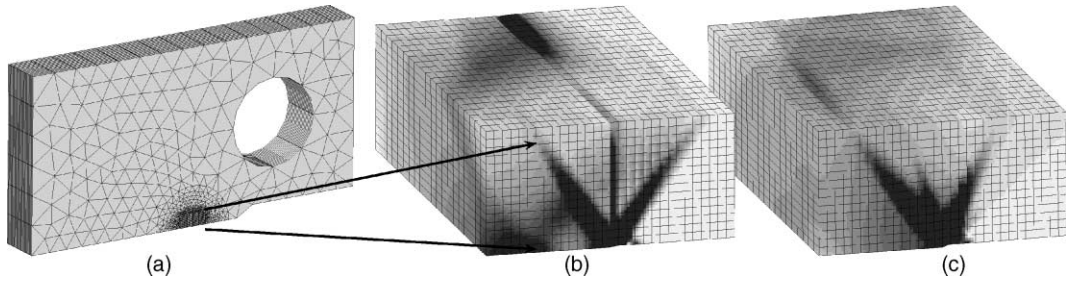

Fig. 7. (a) CT mesh; equivalent plastic deformation field at the crack tip for the $(0\,0\,1)[1\,1\,0]$ (b), and $(0\,0\,1)[1\,0\,0]$ (c) cracks. The visible section corresponds to the interior of the specimen.

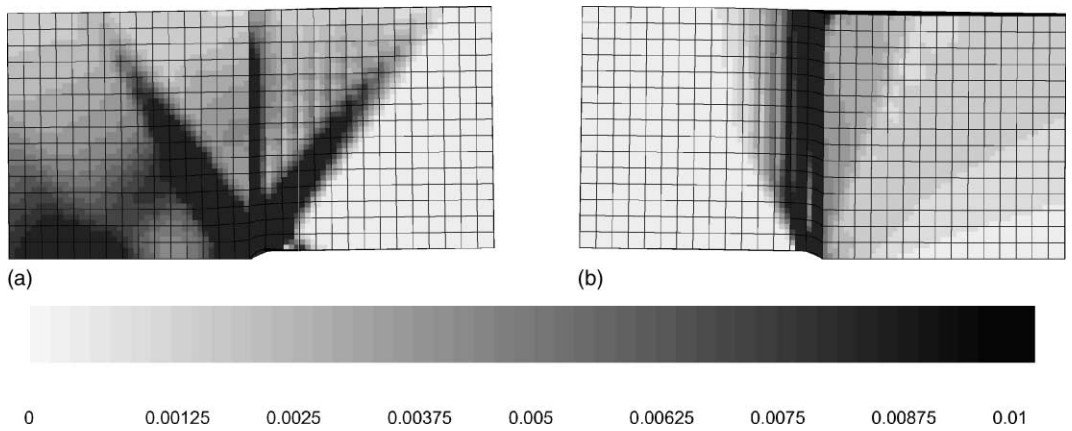

Fig. 8. 3D computation of a single crystal CT specimen: equivalent plastic deformation field. (a) Section in the bulk, (b) outer surface of the specimen ($(0\,0\,1)[1\,1\,0]$ crack).

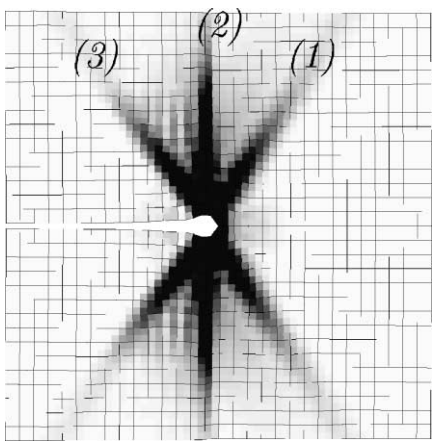

Fig. 9. Crack blunting in a single crystal CT specimen during cyclic loading ($(0\,0\,1)[1\,1\,0]$ crack).

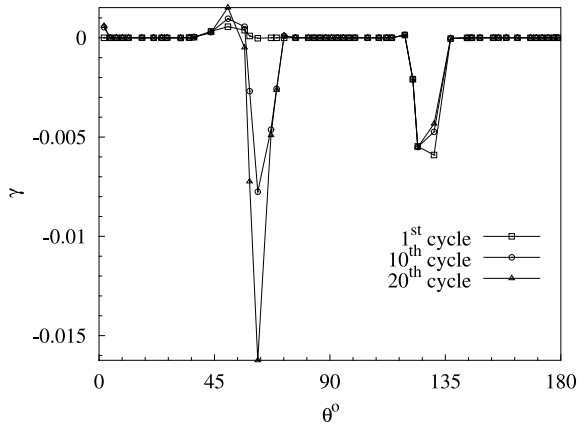

Fig. 10. Activity of slip system $(1\,1\,1)[\bar{1}\,0\,1]$ along a circular line near the crack type at different stages of cyclic deformation ($(0\,0\,1)[1\,1\,0]$ crack).

interpreted as a kink band [15,20]. During subsequent cycles, plastic strains stop accumulating in localization band (3) (at 125°). The active slip system in this latter band then appears in band (1), as shown in Fig. 10. Strain accumulates in the band (1). This results in plastic blunting at the crack tip. The plastic slip variable γ increases by about 0.7% per cycle in band (1). This is associated with non-symmetric stress variation. This local ratchetting phenomenon can be regarded as the origin of fatigue damage. It is thought to play an important role in crack propagation (Fig. 9).

4. Conclusions

Strain localization under cyclic loading has been shown to be related mainly to local ratchetting phenomena. A continuum model for the formation of extrusion in a single crystal plate undergoing single slip has been proposed, based on a non-homogeneous distribution of the kinematic hardening variable. Such fluctuations are likely to appear in cyclically deformed samples and are sufficient to lead to the formation of multiple intense slip bands after cycling. This is also the assumption of micromechanical models like [12]. Note that the proposed continuum model is very different from the one presented in [25], based on the simulation of vacancy diffusion during cyclic loading. Vacancies are associated to dislocation pair annihilation due to the irreversibility of go and fro dislocation motion. It is thought that nonlinear kinematic hardening can be regarded as an effective model for such volume-preserving vacancy diffusion. The advantage of the kinematic hardening model is that a diffusion-mechanical coupling is not necessary.

When a crack initiates in such intense slip bands and grows, it induces a complex stress–strain field, which has been investigated in details via the finite element method. Large scale three-dimensional analyses are necessary because of the important surface effect predicted in a CT specimen. In elastic-perfectly plastic single crystals, three to four localization bands form at the crack tip depending on the orientation. Under cyclic loading, it has been shown that a ratchetting process takes place in the bands ahead of the crack tip, whereas deformation saturates in the others. This feature of cyclic crystal plasticity is expected to play an important role on subsequent crack propagation or branching.

Acknowledgements

This work is supported by Snecma-Moteurs. The authors thank Bertrand Burgardt for stimulating discussions.

References

[1] J.R. Rice, The localization of deformation, in: W.T. Koiter (Ed.), Theoretical and Applied Mechanics, North Publishing Company, 1976.
[2] R.J. Asaro, J.R. Rice, Strain localization in ductile single crystals, J. Mech. Phys. Solids 25 (1977) 309–338.
[3] R.H.J. Peerlings, W.A.M. Brekelmans, R. de Borst, M.G.D. Geers, Gradient-enhanced damage modelling of high-cycle fatigue, Int. J. Numer. Meth. Eng. 49 (2000) 1547–1569.
[4] J.M. Finney, C. Laird, Strain localization in cyclic deformation of copper single crystals, Phil. Mag. 31 (1975) 339–366.
[5] S. Suresh, Fatigue of Materials, Cambridge University Press, 1991.
[6] F. Hanriot, G. Cailletaud, L. Rémy, Mechanical behavior of nickel-base superalloy single crystal, Proc. Int. Conf. High Temp. Constitutive Modeling 1–6 (1991) 139–150.
[7] J.R. Rice, Tensile crack tip fields in elastic-ideally plastic crystals, Mech. Mater. 6 (1987) 317–335.
[8] L. Méric, P. Poubanne, G. Cailletaud, Single crystal modeling for structural calculations: Part 1. Model presentation, J. Eng. Mater. Technol. 113 (1991) 162–170.
[9] K. Tanaka, T. Mura, A dislocation model for fatigue crack initiation, J. Appl. Mech. 48 (1981) 97–103.
[10] R.J. Asaro, Elastic–plastic and kinematic-type hardening, Acta Metal. 223 (1975) 1255–1265.
[11] K. Tanaka, T. Mura, Fatigue crack growth along planar slip bands, Acta Metall. 32 (1984) 1731–1740.
[12] T.H. Lin, K.K.F. Wong, N.J. Teng, Micromechanics of hysteresis loops of fatigue in single crystal, J. Appl. Mech. 67 (2000) 337–343.
[13] J.L. Chaboche, D. Nouailhas, Constitutive modeling of ratchetting effects. Part I: Experiment facts and properties of the classical models, J. Eng. Mater. Technol. 111 (1989) 384–392.
[14] S. Forest, G. Cailletaud, Strain localization in single crystals: Effect of boundaries and interfaces, Eur. J. Mech. A/Solids 14 (5) (1995) 747–771.

[15] J. Rice, D.E. Hawk, R.J. Asaro, Crack tip fields in ductile single crystals, Int. J. Fract. 42 (1990) 301–321.
[16] W.J. Drugan, Asymptotic solutions for tensile crack tip fields without kink-type bands in elastic-ideally plastic single crystals, J. Mech. Phys. Phys. Solids 49 (2001) 2155–2176.
[17] J.R. Rice, Elastic–plastic crack growth, Mechanics of Solids, The R.Hill 60th Anniversary, Vol. 539–562, 1982.
[18] W.J. Drugan, On the asymptotic continuum analysis of quasistatic elastic plastic crack growth and related problems, J. Appl. Mech. 52 (1985) 601–605.
[19] A.M. Cuitiño, M. Ortiz, Computational modeling of single crystals, Modell. Simul. Mater. Sci. Eng. 1 (1992) 225–263.
[20] S. Forest, P. Boubidi, R. Sievert, Strain localization patterns at a crack tip in generalized single crystal plasticity, Scripta Mater. 44 (2001) 953–958.
[21] T.W. Shield, K.-S. Kim, Experimental measurement of the near tip strain field in an iron–silicon single crystal, J. Mech. Phys. Solids 42 (5) (1994) 845–873.
[22] W.C. Crone, T.W. Shield, Experimental study of the deformation near a notch tip in copper and copper beryllium single crystals, J. Mech. Phys. Solids 49 (2001) 2819–2838.
[23] A.M. Cuitiño, M. Ortiz, Three-dimensional crack-tip fields in four-point-bending copper single-crystal specimens, J. Mech. Phys. Solids 44 (1996) 863–904.
[24] F. Feyel, J.-L. Chaboche, FE^2 multiscale approach for the modelling of the elastoviscoplastic behavior of long fibre SiC/Ti composites materials, Comp. Meth. Appl. Mech. Eng. 183 (2000) 309–330.
[25] E.A. Repetto, M. Ortiz, A micromechanical model of cyclic deformation and fatigue-crack nucleation in f.c.c. single crystals, Acta Mater. 45 (1997) 2577–2595.